

# Study of the Family of Glycine–Selenious Acid Addition Compounds: Crystal Structure of Diglycine Hydrogen Selenite and Vibrational Spectra and DSC Measurement of Diglycine Hydrogen Selenite and Monoglycine–Selenious Acid Crystals

Ivan Němec,<sup>1</sup> Ivana Čísařová, and Zdeněk Mička

*Department of Inorganic Chemistry, Charles University, Albertov 2030, 128 40 Prague 2, Czech Republic*

Received December 24, 1997; in revised form April 9, 1998; accepted April 16, 1998

The X-ray structural analysis of diglycine hydrogen selenite has been carried out. The substance crystallizes in the monoclinic space group  $P2_1/c$ ,  $a = 12.2651(7)$ ,  $b = 4.8079(6)$ ,  $c = 19.9550(10)$  Å,  $\beta = 122.745(4)^\circ$ ,  $V = 989.73(14)$  Å<sup>3</sup>,  $Z = 4$ ,  $R = 0.0338$  for 1647 observed reflections. The crystal structure is formed by zwitterions of glycine ( $\text{CH}_2\text{NH}_3^+\text{COO}^-$ ), glycinium cations ( $\text{CH}_2\text{NH}_3^+\text{COOH}$ ), and hydrogen selenite anions ( $\text{HSeO}_3^-$ ) connected by an extensive system of hydrogen bonds. The FTIR and FT Raman spectra of natural and deuterated diglycine hydrogen selenite and monoglycine–selenious acid crystals were recorded and interpreted. The FTIR spectra were studied down to a temperature of 90 K. DSC measurements for both compounds were carried out in the temperature range 95–380 K. No phase transition was found in this temperature range by DSC and FTIR. The existence of ferroelectric properties of diglycine hydrogen selenite and monoglycine–selenious acid crystals can be excluded because of the centrosymmetry of their space groups. © 1998 Academic Press

## INTRODUCTION

Addition compounds of glycine with inorganic acids (i.e., primarily  $\text{H}_2\text{SO}_4$ ,  $\text{H}_2\text{SeO}_4$ ,  $\text{HNO}_3$ , and  $\text{H}_3\text{PO}_4$ ) are formed to a considerable degree by the studied group of compounds. The interest devoted to these compounds is based not only on the fact that it consists of structurally interesting substances, in which the hydrogen bonds play a very important role, but primarily because a number of them exhibit ferroelectric properties. The best known representatives of these ferroelectric substances with short hydrogen bonds are triglycine sulfate (TGS) (1) and diglycine nitrate (DGN) (2). All ferroelectric substances of this type contain a strong hydrogen bond (3) between the carboxyl groups, which

participate in the complex mechanism of the phase transition between the paraelectric and ferroelectric phases.

The submitted work, which is part of our project to search for new potentially ferroelectric substances, is concerned with the study of the addition compounds of glycine and selenious acid. In addition to the compounds of monoglycine–selenious acid (MGSe(IV)) (4), which have already been isolated from the glycine–water–selenious acid system, a further member of this family, diglycine hydrogen selenite (DGSe(IV)), has also been found and studied. The crystal structure of DGSe(IV) and also the vibrational spectra of both compounds and their deuterates have been measured and interpreted. In order to verify the possible existence of phase transitions, FTIR measurements were carried out down to low temperatures and DSC measurements were made in a broad temperature range.

## EXPERIMENTAL

Crystalline DGSe(IV) was prepared by dissolving a mixture (in a molar ratio of 2:1) of glycine (99%, Aldrich) and selenious oxide (Sigma) in water. The 35% solution formed was left to crystallize spontaneously at laboratory temperature. The obtained colorless crystals were collected under vacuum on an S4 frit, washed with ethanol, and dried in the air.

Crystals of MGSe(IV) were prepared and isolated in a similar manner, with the difference that, on the basis of the results of a previous study (4), an input molar ratio of glycine and selenious oxide of 1:2 was used. A modified method of crystallization in tetramethoxysilane (TMS) gel (5) was employed as an alternative method of preparation. An amount of TMS (98%, Fluka) sufficient to ensure that the final mixture contained 10% TMS was added to a 30% aqueous solution of glycine and selenious acid (molar ratio of 4:3). Following mixing on a magnetic stirrer, this clear solution was poured into a test tube, which was closed with

<sup>1</sup>To whom correspondence should be addressed. E-mail: agnemecc@prfdec.natur.cuni.cz.

Parafilm M (American National Can). After 2 weeks, well-developed colorless crystals were formed from the gel (colored red by reduced elemental selenium); these crystals were washed with a mixture of methanol and ethanol (1:1) and dried in the air at laboratory temperature. The crystals obtained were separated into two groups according to shape and were identified as pure glycine and MGSe(IV).

The deuterated compounds ( $\text{CH}_2\text{ND}_3^+\text{COO}^- \cdot \text{D}_2\text{SeO}_3$ ) and ( $\text{CH}_2\text{ND}_3^+\text{COOD} \cdot \text{DSeO}_3^- \cdot \text{CH}_2\text{ND}_3^+\text{COO}^-$ ) were prepared by repeated recrystallization of natural MGSe(IV) and DGSe(IV) from  $\text{D}_2\text{O}$  (99%) in a dessicator over KOH.

The contents of carbon, nitrogen, and hydrogen were determined using a Perkin–Elmer 240 C elemental analyzer.

The infrared spectra of nujol and fluorolube mulls were recorded on an ATI Mattson Genesis FTIR spectrometer ( $2\text{ cm}^{-1}$  resolution, Beer–Norton medium apodization) in the  $400\text{--}4000\text{ cm}^{-1}$  region. Low-temperature measurements were carried out using the nujol mull method in low-temperature cell with KBr windows in the  $298\text{--}90\text{ K}$  interval. The temperature was controlled by a Fe–Const. thermocouple. The analog signal was processed on a PC using the AX5232 temperature measurement board.

The Raman spectra of polycrystalline samples were recorded on a Bruker RFS 100 FT Raman spectrometer ( $2\text{ cm}^{-1}$  resolution, Blackman–Harris 4-Term apodization,  $1064\text{ nm}$  NdYAG laser excitation,  $150\text{ mW}$  power at the sample) in the  $50\text{--}4000\text{ cm}^{-1}$  region.

The DSC measurements were carried out on a Perkin–Elmer DSC 7 power-compensated apparatus in the  $95\text{--}380\text{ K}$  temperature region (helium or nitrogen atmosphere). A heating rate of  $10\text{ K min}^{-1}$  was selected to measure approximately  $10\text{ mg}$  of finely ground sample placed in aluminium capsule.

The X-ray data collection for the DGSe(IV) single crystal was carried out on an Enraf–Nonius CAD4-MACH III four-circle diffractometer (MoK $\alpha$ , graphite monochromator). The phase problem was solved by direct methods and the nonhydrogen atoms were refined anisotropically, using the full-matrix least-squares procedure. The H atom positions were found from the difference Fourier map and their displacement factors were refined isotropically. The basic crystallographic data and the details of the measurement and refinement are summarized in Table 1. A list of the observed and calculated structural factors and the anisotropic displacement factors are available from the authors upon request.

## RESULTS AND DISCUSSION

### The Crystal Structure of DGSe(IV)

The atomic coordinates are given in Table 2, and the bond lengths and angles, including those for the hydrogen bonds, are listed in Table 3. The atom numbering can be seen in Fig. 1 and the packing scheme is depicted in Fig. 2.

**TABLE 1**  
Basic Crystallographic Data, Data Collection, and Refinement Parameters

Empirical formula	$\text{C}_4\text{H}_{12}\text{N}_2\text{O}_7\text{Se}$
<i>a</i>	12.2651(7) Å
<i>b</i>	4.8079(6) Å
<i>c</i>	19.9550(10) Å
$\beta$	122.745(4)°
<i>V</i>	989.73(14) Å <sup>3</sup>
<i>Z</i>	4
<i>D</i> (calc.)	1.873 Mg m <sup>-3</sup>
Crystal system	monoclinic
Space group	$P2_1/c$
<i>M<sub>r</sub></i>	279.12
$\mu(\text{MoK}\alpha)$	3.811 mm <sup>-1</sup>
<i>F</i> (000)	560
Crystal dimensions	0.6 × 0.2 × 0.05 mm
Crystal form	plate
Diffractometer and radiation used	Enraf–Nonius CAD4-MACH III, MoK $\alpha$ , $\lambda = 0.71069\text{ Å}$
Scan technique	$\omega$ -2 $\theta$
Number and $\theta$ range of reflections for lattice parameter refinement	25, 13–15°
Range of <i>h</i> , <i>k</i> , and <i>l</i>	–14 → 15, 0 → 5, –24 → 24
Number of standard reflections	3
Standard reflections monitored in interval	60 min.
Intensity decrease	4.6%
Total number of reflections measured	3621
$\theta$ range	1.97–25.97°
Number of independent reflections ( <i>R</i> <sub>int</sub> )	1935 (0.021)
Number of observed reflections	1647
Criterion for observed reflections	$I > 2\sigma(I)$
Absorption correction	analytical from crystal shape
<i>T</i> <sub>min</sub>	0.481
<i>T</i> <sub>max</sub>	0.829
Function minimized	$\sum w(F_o^2 - F_c^2)^2$
Weighting scheme	$w = [\sigma^2(F_o^2) + (0.0332P)^2 + 2.94P]^{-1}$ $P = (F_o^2 + 2F_c^2)/3$
Parameters refined	175
Value of <i>R</i>	0.0338
Value of <i>wR</i>	0.0958
Value of <i>S</i>	1.286
Maximum and minimum heights in final $\Delta\rho$ map	0.891, –0.635 e. Å <sup>-3</sup>
Source of atomic scattering factors	SHELXL93 (28), International Tables for X-ray Crystallography (29)
Programs used	SHELXL93 (28), JANA96 (30), PARST (31), PLUTO (32)

The crystal structure consists of glycine zwitterions ( $\text{CH}_2\text{NH}_3^+\text{COO}^-$ ), glycinium cations ( $\text{CH}_2\text{NH}_3^+\text{COOH}$ ), and hydrogen selenite anions ( $\text{HSeO}_3^-$ ) connected by an extensive system of hydrogen bonds (see Table 3).

In addition to the discovery of hydrogen atoms H21 at a bonding distance from atom O21, also the length of the

TABLE 2

Fractional Atomic Coordinates ( $\times 10^4$ ) and Equivalent (for Non-H Atoms  $\times 10^3$ ) or Isotropic (for H Atoms  $\times 10^3$ ) Displacement Factors with Standard Deviations in Brackets  $U_{\text{eq}} = 1/3 \sum_i \sum_j U_{ij} a_i^* a_j^* a_i a_j$

	x	y	z	$U_{\text{eq}}$ ( $\text{\AA}^2$ )
Se	2419(1)	944(1)	1089(1)	23(1)
O1	2132(3)	906(7)	1814(2)	28(1)
O2	4012(3)	1106(7)	1552(2)	33(1)
O3	2141(4)	−2663(8)	844(2)	37(1)
O11	6716(3)	236(8)	1615(2)	33(1)
O12	7970(3)	2372(8)	520(2)	34(1)
O21	6469(4)	−1387(8)	488(2)	36(1)
O22	9449(3)	1728(7)	1812(2)	33(1)
C11	6281(4)	−1422(9)	1077(3)	25(1)
C12	8995(4)	3016(10)	1185(3)	23(1)
C21	5440(5)	−3828(11)	1003(3)	28(1)
C22	9688(4)	5588(10)	1157(3)	26(1)
N1	5327(4)	−3932(9)	1702(2)	26(1)
N2	10935(4)	5973(9)	1918(2)	24(1)
H3	2052(53)	−2765(134)	382(36)	42(16)
H21	7040(79)	367(192)	539(50)	98(28)
H121	5833(62)	−5513(147)	991(37)	55(18)
H122	9880(49)	5369(114)	730(31)	33(14)
H221	4616(59)	−3757(125)	554(36)	46(17)
H222	9092(53)	6982(132)	1081(32)	41(16)
H1N1	6090(52)	−3995(109)	2147(32)	27(13)
H2N1	4860(56)	−5589(133)	1665(34)	42(16)
H3N1	4913(65)	−2222(170)	1753(40)	65(20)
H1N2	11447(46)	4623(112)	1998(27)	18(12)
H2N2	10764(58)	5917(132)	2276(39)	50(18)
H3N2	11297(53)	7783(139)	1896(32)	40(15)

C11–O11 (1.206 Å) and C11–O21 (1.314 Å) bonds confirm the presence of glycinium in the structure. The bonding distances in the deprotonized carboxyl group of the zwitterion of glycine have values of 1.226 Å (C12–O22) and 1.277 Å (C12–O12). The marked lengthening of the C12–O12 bond is apparently caused by participation of the O12 atom in two of the shortest hydrogen bonds in the structure (2.556 and 2.655 Å), which connect the glycine zwitterion to the glycinium cation and the hydrogen selenite anion, respectively.

The determined bonding angles in the  $\text{NH}_3^+$  group lie in the 106–112° interval. The reason why the expected tetrahedral symmetry of these groups is somewhat disturbed probably lies in the intense participation of the protons in the hydrogen bond system of the N–H...O type (see Table 3). Only linear (two-center) hydrogen bonds were found for the  $\text{NH}_3^+$  group in the crystal structure of DGSe(IV), similar to MGSe(IV) (4). In contrast to some related compounds of glycine (6–8), no bifurcated (three-center) hydrogen bond was found.

The glycine and glycinium molecules are practically planar in the structure and only the nitrogen atoms are bent

TABLE 3  
Bond Lengths (Å) and Selected Angles (°)

Se–O1	1.663(3)	O2–Se–O1	104.9(2)
Se–O2	1.651(3)	O2–Se–O3	101.1(2)
Se–O3	1.784(4)	O1–Se–O3	97.4(2)
		Se–O3–H3	104(4)
C11–O11	1.206(6)	O11–C11–O21	125.6(4)
C11–O21	1.314(5)	O11–C11–C21	123.0(4)
C11–C21	1.503(6)	O21–C11–C21	111.4(4)
C21–N1	1.476(6)	N1–C21–C11	110.1(4)
C21–H121	0.95(7)	N1–C21–H121	108(4)
C21–H221	0.92(6)	C11–C21–H121	109(4)
C12–O22	1.226(5)	N1–C21–H221	108(4)
C12–O12	1.277(5)	C11–C21–H221	114(4)
C12–C22	1.519(6)	H121–C21–H221	108(5)
C22–N2	1.471(6)	C11–O21–H21	110(5)
C22–H122	1.01(5)	C21–N1–H1N1	111(3)
C22–H222	0.94(6)	C21–N1–H2N1	108(3)
		H1N1–N1–H2N1	108(5)
		C21–N1–H3N1	112(4)
		H1N1–N1–H3N1	104(5)
		H2N1–N1–H3N1	112(5)
		O22–C12–O12	125.8(4)
		O22–C12–C22	119.6(4)
		O12–C12–C22	114.6(4)
		N2–C22–C12	110.8(4)
		N2–C22–H122	107(3)
		C12–C22–H122	110(3)
		N2–C22–H222	111(3)
		C12–C22–H222	101(4)
		H122–C22–H222	117(5)
		C22–N2–H1N2	110(3)
		C22–N2–H2N2	106(4)
		H1N2–N2–H2N2	108(5)
		C22–N2–H3N2	108(3)
		H1N2–N2–H3N2	112(4)
		H2N2–N2–H3N2	113(5)

## Hydrogen bonds

Donor–H	Donor...Acceptor	H...Acceptor	Donor–H...Acceptor
O21–H21	O21...O12	H21...O12	O21–H21...O12
1.07(9)	2.556(6)	1.51(0)	166(7)
N1–H1N1	N1...O1 <sup>i</sup>	H1N1...O1 <sup>i</sup>	N1–H1N1...O1 <sup>i</sup>
0.87(5)	2.916(6)	2.04(6)	179(4)
N1–H2N1	N1...O2 <sup>ii</sup>	H2N1...O2 <sup>ii</sup>	N1–H2N1...O2 <sup>ii</sup>
0.96(6)	2.803(6)	1.85(7)	176(4)
N1–H3N1	N1...O2	H3N1...O2	N1–H3N1...O2
1.00(8)	2.835(6)	1.86(8)	164(4)
N2–H1N2	N2...O1 <sup>iii</sup>	H1N2...O1 <sup>iii</sup>	N2–H1N2...O1 <sup>iii</sup>
0.86(5)	2.910(6)	2.09(6)	160(4)
N2–H2N2	N2...O22 <sup>iv</sup>	H2N2...O22 <sup>iv</sup>	N2–H2N2...O22 <sup>iv</sup>
0.85(7)	2.842(6)	2.01(7)	166(5)
N2–H3N2	N2...O1 <sup>v</sup>	H3N2...O1 <sup>v</sup>	N2–H3N2...O1 <sup>v</sup>
0.99(7)	2.855(6)	1.88(7)	171(4)
O3–H3	O3...O12 <sup>vi</sup>	H3...O12 <sup>vi</sup>	O3–H3...O12 <sup>vi</sup>
0.87(6)	2.655(5)	1.80(7)	169(5)

## Equivalent positions

- (i)  $-x + 1, y - 1/2, -z + 1/2$  (iv)  $-x + 2, y + 1/2, -z + 1/2$   
(ii)  $x, y - 1, z$  (v)  $x + 1, y + 1, z$   
(iii)  $x + 1, y, z$  (vi)  $-x + 1, -y, -z$

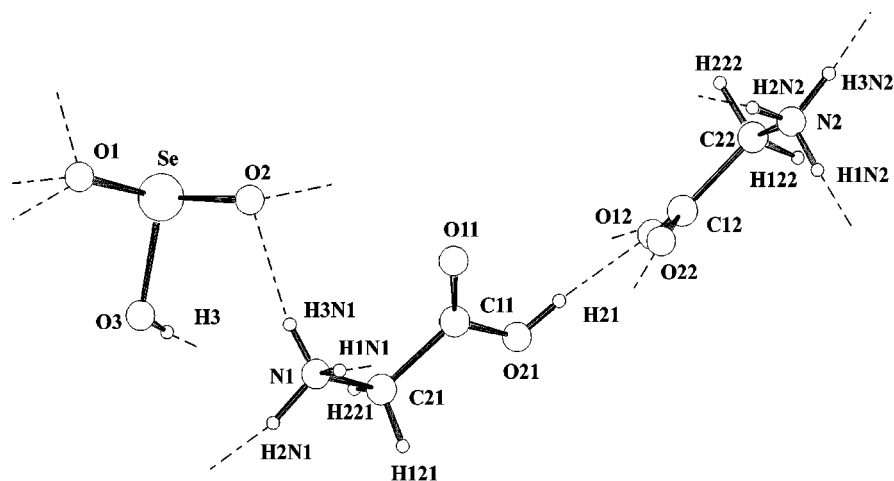


FIG. 1. Asymmetric unit of DGSe(IV). Dashed lines indicate hydrogen bonds.

out of the plane defined by the O11, O21, C11, C21 (glycinium) and O12, O22, C12, C22 (glycine) atoms by 0.102 and 0.159 Å, respectively (see Table 4). The corresponding torsion angles O11–C11–C21–N1 and O22–C12–C22–N2 have values of 4.2 and 5.8°. Conditions for MGSe(IV) (4) differ in that nitrogen has a greater impact in disturbing the planarity of the glycine zwitterion (the O–C–C–N torsion angle has a value of 15.3°). These results, together with information from earlier studies (1, 9, 10), confirm that the planarity of the glycine molecule does not depend on its ionic state.

The lengths of the Se–O (1.663 and 1.651 Å) and Se–O(H) (1.784 Å) bonds are quite appropriate for the hydrogen

selenite anion (11, 12). Slight differences in the Se–O bond lengths together with the slight deformation of the anions indicate a different manner of connection of the oxygen atoms in the hydrogen bond system in the DGSe(IV) crystal structure (see Table 3).

#### Analysis of the Vibrational Spectra

The number of normal modes of the MGSe(IV) and DGSe(IV) crystals was determined by nuclear site group analysis (13). Standard correlation methods (14) were used for more detailed study of the expected vibrational features of the  $\text{H}_2\text{SeO}_3$  and  $\text{HSeO}_3^-$  groups. The results obtained are presented in Tables 5–7.

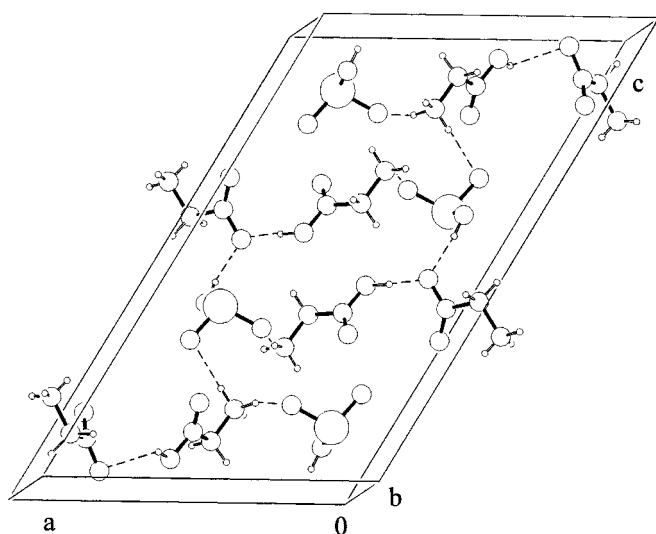


FIG. 2. Packing scheme of DGSe(IV). Dashed lines indicate hydrogen bonds.

TABLE 4  
Analysis of the Planarity of Glycinium and Glycine Molecules in DGSe(IV)

Equations of the planes			
Glycinium	$7.64x - 2.74y + 2.27z = 5.43$		
Glycine	$9.70x - 2.71y - 12.47z = 6.44$		
Atomic deviations (Å)			
Glycinium		Glycine	
O11	0.000	O12	0.002
O21	0.000	O22	0.003
C11	0.000	C12	-0.007
C21	0.000	C22	0.002
N1 <sup>a</sup>	0.102	N2 <sup>a</sup>	0.159

<sup>a</sup> Atom not used to define plane.

TABLE 5

The Results of the Nuclear Site Group Analysis for MGSe(IV)

	$C_{2h}^5$	$A_g$	$A_u$	$B_g$	$B_u$
	Acoustical		1		2
External modes	Translational	6	5	6	4
	Librational	6	6	6	6
Internal modes		36	36	36	36
	Total	48	48	48	48
Activity		RA(xx, yy, zz, xy)	IR(z)	RA(xz, yz)	IR(x, y)

Monoclinic MGSe(IV) (4) crystals belong in the  $P2_1/n$  ( $C_{2h}^5$ ) space group with 16 atoms in the asymmetric unit of the unit cell ( $Z = 4$ ). All the atoms occupy four-fold positions  $e(C_1)$ . Two types of species present in the unit cell,  $H_2SeO_3$  and  $CH_2NH_3^+COO^-$ , occupying four-fold positions  $e(C_1)$ , were considered in more detailed calculations of the internal and external modes.

As is apparent from the first part of our discussion, DGSe(IV) crystals belong in space group  $P2_1/c$  ( $C_{2h}^5$ ) with 26 atoms in the asymmetric unit of the unit cell ( $Z = 4$ ). All the atoms once again occupy four-fold positions  $e(C_1)$ . In a more detailed analysis, three types of particles present,  $CH_2NH_3^+COOH$ ,  $HSeO_3^-$ , and  $CH_2NH_3^+COO^-$ , occupying four-fold positions  $e(C_1)$ , were considered in the unit cell.

Following a certain degree of simplification (the OH groups are considered to be a single atom), the  $H_2SeO_3$  and  $HSeO_3^-$  species can be considered to be pyramidal molecules of the  $ZXY_2$  type with symmetry corresponding to point group  $C_s$ . As the symmetry of the MGSe(IV) and DGSe(IV) is characterized by factor group  $C_{2h}^5$  and both species occupy

TABLE 6

The Results of the Nuclear Site Group Analysis for DGSe(IV)

	$C_{2h}^5$	$A_g$	$A_u$	$B_g$	$B_u$
	Acoustical		1		2
External modes	Translational	9	8	9	7
	Librational	9	9	9	9
Internal modes		60	60	60	60
	Total	78	78	78	78
Activity		RA(xx, yy, zz, xy)	IR(z)	RA(xz, yz)	IR(x, y)

four-fold positions in the structures, with site symmetry  $C_1$ , more detailed study of the expected vibrational manifestations of both species  $H_2SeO_3$  and  $HSeO_3^-$  can be carried out simultaneously (Table 7).

In agreement with the results of nuclear site group analysis, the vibrational spectra of DGSe(IV) were found to contain far more bands than for MGSe(IV). The results of the analyses indicate the expected splitting of all the bands into doublets in the IR and Raman spectra. This splitting was observed only for some bands, especially in low-temperature IR spectra. This fact could be explained both by small coupling between adjacent species and also in terms of the fact that all the measurements were carried out with polycrystalline samples, where the splitting of the vibrational bands is harder to observe.

Vibrational Spectra of MGSe(IV)

The IR spectra of MGSe(IV) recorded at laboratory and low temperatures (90 K), together with the Raman spectrum

TABLE 7  
Correlation Analysis of  $H_2SeO_3$  and  $HSeO_3^-$  Internal Modes in MGSe(IV) and DGSe(IV) Crystals

Pyramidal molecule $ZXY_2^a$	Degrees of freedom	Free molecule symmetry $C_s$	Site symmetry $C_1$	Factor group symmetry $C_{2h}$	Vibration modes	Activity	
$v_1$ $\nu(XZ)$	4	$A'$	$A$	$A_g$	$\nu_1, \nu_2, \nu_3, \nu_4, \nu_5, \nu_6$	RA(xx, yy, zz, xy)	
$v_2$ $\nu_s(XY)$	4			$A_u$	$\nu_1, \nu_2, \nu_3, \nu_4, \nu_5, \nu_6$	IR(z)	
$v_3$ $\delta_s(YXZ)$	4			$B_g$	$\nu_1, \nu_2, \nu_3, \nu_4, \nu_5, \nu_6$	RA(xz, yz)	
$v_4$ $\delta(YXY)$	4			$B_u$	$\nu_1, \nu_2, \nu_3, \nu_4, \nu_5, \nu_6$	IR(x, y)	
$v_5$ $\nu_a(XY)$	4	$A''$					
$v_6$ $\delta_d(YXZ)$	4						

<sup>a</sup>According to Nakamoto (19) the OH groups were assumed to be single atoms.

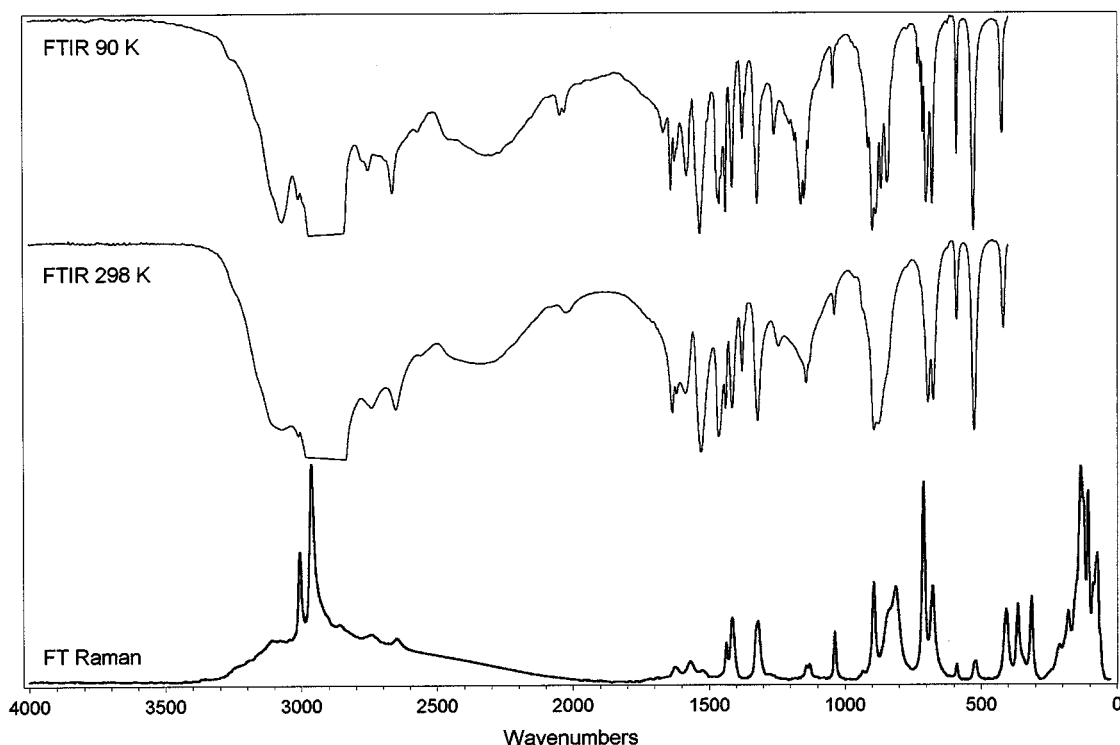


FIG. 3. FTIR (nujol mull) and FT Raman spectra of MGSe(IV).

are depicted in Fig. 3 and the absorption maxima are listed in Table 8. The absorption maxima observed in the IR and Raman spectra of the deuterated analog are given in Table 9. The overall character of the vibrational spectra of MGSe(IV) is fully in accord with the results of solution of the crystal structure of this addition compound (4), which is formed of molecules of selenious acid and glycine in the form of the  $\text{CH}_2\text{NH}_3^+\text{COO}^-$  zwitterion interconnected by a system of hydrogen bonds.

The assignment of the bands in the vibrational spectra of MGSe(IV) and its deuterates was based on the results of previous studies on the interpretation of the spectra of  $\alpha$ -glycine (15–17), selenious acid (18–20), and the addition compounds of glycine (21–23).

Broad, intense bands in the IR spectrum in the 3200–2100  $\text{cm}^{-1}$  region are characteristic for the stretching vibrations of the N–H and O–H groups connected in hydrogen bonds in a crystal. It is apparent from the crystal structure that these are hydrogen bonds of the N–H...O type with a length of 2.8–2.9 Å and of the O–H...O type with a length of  $\sim 2.6$  Å. As expected, these bands were correspondingly shifted to the 2400–1700  $\text{cm}^{-1}$  region in the deuterate.

The “indicator band” at 2020  $\text{cm}^{-1}$  in the IR spectrum is an important indication of the presence of the  $\text{NH}_3^+$  group in the compound (21, 22). This band is a combination of the antisymmetric deformation vibration and torsion vibration of the  $\text{NH}_3^+$  group. An increase in its intensity, accompanied

by splitting into two symmetrical components (2046 and 2030  $\text{cm}^{-1}$ ), can be observed in the low-temperature IR spectrum.

The pair of bands at  $\sim 1630$  and  $\sim 1620$   $\text{cm}^{-1}$  can be interpreted as corresponding to the antisymmetric deformation vibration of the  $\text{NH}_3^+$  group. The observed splitting is not only in agreement with the results of nuclear site group analysis (see Table 5), but is also in accord with the results of calculation of the normal vibrations of  $\alpha$ -glycine (15). As the temperature decreases, a further splitting of these bands can be observed in the IR spectrum. Confirmation of the expected assignment was also found in a decrease in the wavenumbers of the bands for the deuterated compounds (1172 and 1164  $\text{cm}^{-1}$ ).

The medium-intensity band at 1585  $\text{cm}^{-1}$  in the IR spectrum or 1569  $\text{cm}^{-1}$  in the Raman spectrum can be assigned to the antisymmetric stretching vibrations of the  $\text{COO}^-$  group, similar as for  $\alpha$ -glycine (15, 17). Although this band can be found in the 1615–1635  $\text{cm}^{-1}$  region for a number of addition compounds of glycine (21, 22), the fact that practically no shift was observed on deuteration provides support for our interpretation.

A temperature dependence was observed for the band of the deformation vibration of the SeOH group (1244  $\text{cm}^{-1}$ ). During cooling, the absorption maximum is shifted to higher wavenumbers (by 15  $\text{cm}^{-1}$ ) and the band intensity also changes. Similar changes have also been observed for some hydrogen selenites (12, 24).

**TABLE 8**  
**FTIR and FT Raman Spectra of MGSe(IV)**

Assignment	IR			Assignment	IR		
	298 K	90 K	Raman		298 K	90 K	Raman
$\nu$ O–H...O, $\nu$ N–H...O	3245 sh	3260 sh		$\rho$ NH <sub>3</sub> <sup>+</sup>	1143 m	1148 s	1141 w
	3155 sh	3160 sh	3110 w		1130 m	1134 m	1129 w
	3070 mb	3068 m			1113 sh	1100 sh	
$\nu_{as}$ CH <sub>2</sub>	3009 w	3008 w	3007 s	$\nu$ C–N	1038 w	1043 m	1037 m
$\nu_s$ CH <sub>2</sub>	2983 w	n.o. <sup>a</sup>	2964 vs	$\rho$ CH <sub>2</sub>	934 sh	940 sh	934 w
$\nu$ O–H...O, $\nu$ N–H...O	2900 mb	n.o. <sup>a</sup>	2905 sh			914 m	927 w
	2845 m	n.o. <sup>a</sup>	2858 w				
		2770 m		$\nu$ C–C	894 s	898 s	894 s
	2740 m	2753 m	2740 w			886 s	
		2690 w		$\nu$ Se–O ( $\nu_1$ H <sub>2</sub> SeO <sub>3</sub> )	876 s	866 s	838 s
	2650 m	2662 m	2650 w		846 sh	845 s	812 s
	2560 w	2570 w		?		733 w	
		2450 mb		$\delta$ COO <sup>–</sup>	710 sh	714 m	
$\delta_{as}$ NH <sub>3</sub> <sup>+</sup> + $\tau$ NH <sub>3</sub> <sup>+</sup>	2350 sb	2310 sb		$\nu_s$ Se–OH ( $\nu_2$ H <sub>2</sub> SeO <sub>3</sub> ), $\delta$ COO <sup>–</sup>			711 vs
		2046 m		$\nu_s$ Se–OH ( $\nu_2$ H <sub>2</sub> SeO <sub>3</sub> )	694 s	701 s	
	2020 wb	2030 m		$\nu_{as}$ Se–OH ( $\nu_5$ H <sub>2</sub> SeO <sub>3</sub> )	675 s	678 s	677 s
$\delta_{as}$ NH <sub>3</sub> <sup>+</sup>		1665 m		$\omega$ COO <sup>–</sup>	589 w	589 m	589 w
	1633 s	1637 s	1627 w	$\rho$ COO <sup>–</sup>	525 s	527 s	520 w
	1619 s	1625 m	1618 w	$\delta_s$ HO–Se–O	417 w	422 m	407 s
		1614 sb		( $\nu_3$ H <sub>2</sub> SeO <sub>3</sub> ), $\tau$ NH <sub>3</sub> <sup>+</sup>			
$\nu_{as}$ COO <sup>–</sup>	1585 m	1579 s	1569 w	$\delta$ C–C–N, $\delta_{as}$ HO–Se–O			364 s
$\delta_s$ NH <sub>3</sub> <sup>+</sup>	1528 s	1531 s	1522 w	( $\nu_6$ H <sub>2</sub> SeO <sub>3</sub> )			
sci CH <sub>2</sub>	1437 s	1438 s	1436 m	$\delta$ HO–Se–OH ( $\nu_4$ H <sub>2</sub> SeO <sub>3</sub> )			314 s
$\nu_s$ COO <sup>–</sup>	1415 s	1414 s	1414 s	lattice modes			210 w
$\omega$ CH <sub>2</sub>			1325 m				179 s
	1320 s	1321 s	1319 s				150 sh
$\delta$ Se–O–HOHO	1244 m	1259 m					134 vs
		1202 w					122 s
	1165 sh	1184 w					106 s
$\rho$ NH <sub>3</sub> <sup>+</sup>		1161 s					87 s
							78 s
							71 s
							60 w

<sup>a</sup>Not observed due to nujol bands.

Note. Abbreviations: vs, very strong; s, strong; m, medium; w, weak; b, broad; sh, shoulder;  $\nu$ , stretching;  $\delta$ , deformation or in-plane bending;  $\omega$ , wagging;  $\tau$ , torsional;  $\gamma$ , out-of-plane bending;  $\rho$ , rocking; sci, scissoring; twi, twisting; s, symmetric; as, antisymmetric.

The expected splitting of the internal modes of the H<sub>2</sub>SeO<sub>3</sub> group (see Table 7) was observed only for the  $\nu_1$  vibration in the IR and Raman spectra. Following deuteration, this splitting can no longer be observed at laboratory temperature.

Lattice modes appear in the 200 to 60 cm<sup>–1</sup> region in the Raman spectra of MGSe(IV) and its deuterated analogs. The intense vibrations at 134 and 106 cm<sup>–1</sup> can be assigned to the torsion vibrations of the COO<sup>–</sup> (15) and C–C (16) groups.

#### Vibrational Spectra of DGSe(IV)

The IR spectra of DGSe(IV) recorded at laboratory and low temperatures (90 K), together with the Raman spectrum are depicted in Fig. 4, and the absorption maxima are given in Table 10. The absorption maxima observed in the IR and Raman spectra of the deuterated analog are given in Table 11. The overall character of the vibrational spectra is in accord with the results of solution of the crystal structure of a compound consisting of molecules of glycine in the form of

TABLE 9  
FTIR and FT Raman Spectra of Deuterated MGSe(IV)

Assignment	IR	Raman	Assignment	IR	Raman
?	3105 w		$\nu$ CN, $\nu$ CC, $\rho$ ND <sub>3</sub> <sup>+</sup>	973 w	972 m
$\nu_{\text{as}}$ CH <sub>2</sub>	3006 w	3007 s	$\delta$ Se–O–D	900 sh	
$\nu_{\text{s}}$ CH <sub>2</sub>	2961 w	2964 vs	$\nu$ Se–O ( $\nu_1$ D <sub>2</sub> SeO <sub>3</sub> )	869 s	842 vs
?	2905 wb		$\nu$ CN, $\nu$ CC, $\rho$ ND <sub>3</sub> <sup>+</sup>	821 m	
2 × sci CH <sub>2</sub> ?	2864 wb	2855 w	$\rho$ CH <sub>2</sub> , $\rho$ ND <sub>3</sub> <sup>+</sup>	792 m	
?	2790 wb		?	715 sh	
$\nu$ N–D...O, $\nu$ O–D...O	2380 sh	2383 m	$\nu_{\text{s}}$ Se–OD ( $\nu_2$ D <sub>2</sub> SeO <sub>3</sub> )	692 sh	694 vs
	2341 m	2344 m	$\nu_{\text{as}}$ Se–OD ( $\nu_5$ D <sub>2</sub> SeO <sub>3</sub> )	681 s	676 s
	2313 m	2315 m	$\delta$ COO <sup>−</sup>	653 m	653 m
				612 w	
	2262 m	2265 m	$\omega$ COO <sup>−</sup>	576 w	583 w
	2227 m		$\rho$ COO <sup>−</sup>	509 s	505 w
	2172 m	2177 m	$\delta_{\text{s}}$ DO–Se–O ( $\nu_3$ D <sub>2</sub> SeO <sub>3</sub> )	408 w	401 s
	2130 m		$\delta$ C–C–N, $\delta_{\text{as}}$ DO–Se–O		359 s
	1970 m	1970 sh	( $\nu_6$ D <sub>2</sub> SeO <sub>3</sub> )		
			$\delta$ DO–Se–OD ( $\nu_4$ D <sub>2</sub> SeO <sub>3</sub> )		308 s
	1770 wb		lattice modes		216 w
$\nu_{\text{as}}$ COO <sup>−</sup>	1580 s	1570 w			178 w
sci CH <sub>2</sub>	1435 s	1434 m			156 m
$\nu_{\text{s}}$ COO <sup>−</sup>	1411 s	1411 s			134 vs
$\omega$ CH <sub>2</sub>	1310 s	1311 m			122 s
twi CH <sub>2</sub>	1277 m	1277 m			106 s
$\delta_{\text{s}}$ ND <sub>3</sub> <sup>+</sup>	1188 m	1188 w			86 s
					77 s
$\delta_{\text{as}}$ ND <sub>3</sub> <sup>+</sup>	1172 m	1173 w			71 s
	1164 m				61 m
$\rho$ CH <sub>2</sub> , $\rho$ ND <sub>3</sub> <sup>+</sup>	1045 w				
$\nu$ CN, $\nu$ CC, $\rho$ ND <sub>3</sub> <sup>+</sup>		1010 m			

a zwitterion, (CH<sub>2</sub>NH<sub>3</sub><sup>+</sup>COO<sup>−</sup>), and glycinium (CH<sub>2</sub>NH<sub>3</sub><sup>+</sup>COOH) together with the hydrogen selenite anion (HSeO<sub>3</sub><sup>−</sup>). These structural units are interconnected by an extensive network of hydrogen bonds (see Table 3).

Assignment of the bands in the vibrational spectra of DGSe(IV) and its deuterate was once again based on the results of studies of the vibrational spectra of  $\alpha$ -glycine (15–17), hydrogen selenites (18–20), and addition compounds of glycine (21–23, 25, 26).

The valence vibrations of the N–H and O–H groups interconnected by a system of hydrogen bonds in a crystal appear in the IR spectrum as broad bands in the 3200–1800 cm<sup>−1</sup> region. As can be seen from Table 3, these consist of hydrogen bonds of the N–H...O type with a length of approximately 2.8 to 2.9 Å and O–H...O type with lengths of 2.56 and 2.66 Å. The bands in the 2400–1800 cm<sup>−1</sup> interval can be assigned analogously for the deuterated compounds.

The stretching vibration of the CH<sub>2</sub> group can be observed in the 3014–2950 cm<sup>−1</sup> region in the Raman spectra

and IR spectrum of the deuterate. Its splitting into doublets is apparently caused by the presence of two nonequivalent glycine forms in the crystal. Similar splitting has also been observed in the spectra of other addition compounds of glycine (21, 22). In the IR spectra of the natural molecules these bands are almost overlapped by the bands of the stretching N–H and O–H vibrations.

The presence of the NH<sub>3</sub><sup>+</sup> group in the compound is also confirmed by the combination “indicator band” (21, 22) at 2100 cm<sup>−1</sup> in the IR spectrum. A decrease in the temperature to 90 K is accompanied by an increase in its intensity and a shift to higher wavenumbers by 19 cm<sup>−1</sup>.

The broad, quite weak band in the 2040–1870 cm<sup>−1</sup> region could be interpreted as a further branch of the stretching O–H vibration. On the basis of correlation curves (27) between the wavenumber of the vibration and the length of the hydrogen bond, these bands would indicate the presence of hydrogen bonds with a length of 2.53 to 2.54 Å; however, such bonds were not found in the crystal structure.



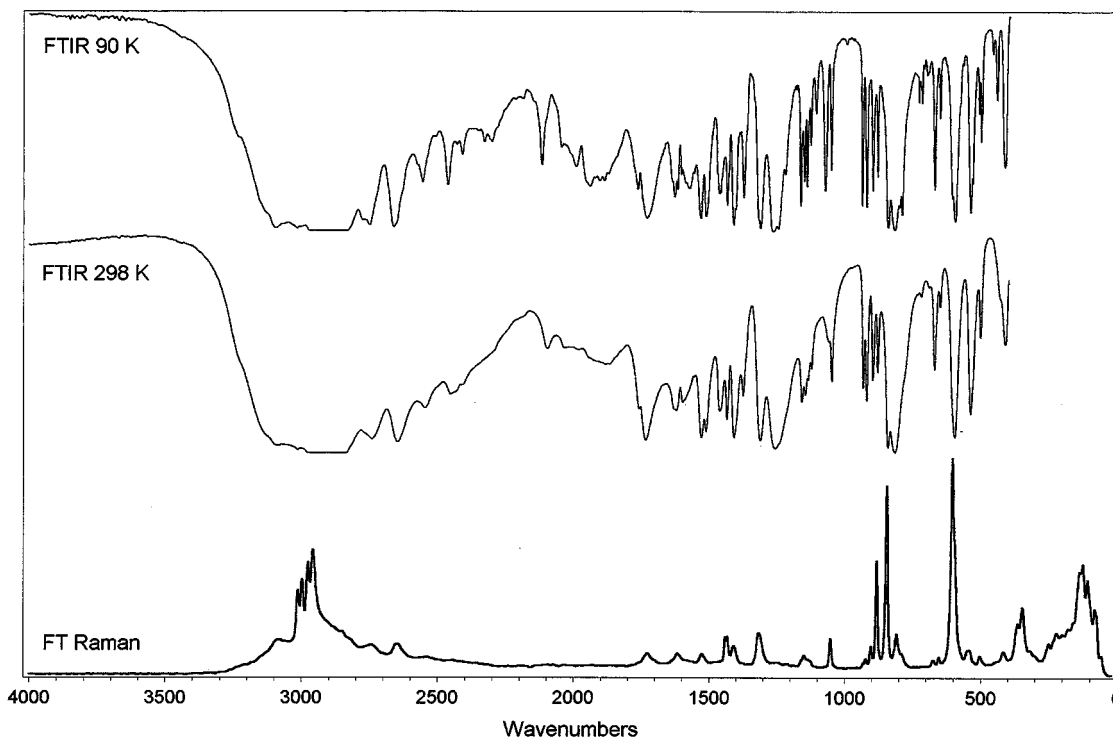


FIG. 4. FTIR (nujol mull) and FT Raman spectra of DGSe(IV).

The C=O stretching vibrations, indicating the presence of the glycinium cation ( $\text{CH}_2\text{NH}_3^+\text{COOH}$ ), are manifested in a band at  $\sim 1730\text{ cm}^{-1}$ . The splitting of this band (the less intense component lies at  $\sim 1760\text{ cm}^{-1}$ ) is in accord with the results of nuclear site group analysis (Table 6); however, this phenomenon could also be explained by Fermi interactions between the C=O valence vibrations and the first overtone of the symmetric C-C valence vibration (21, 22).

The pair of medium-intensity bands in the IR spectrum at  $\sim 1630\text{ cm}^{-1}$  and  $\sim 1620\text{ cm}^{-1}$  (a weak band at  $1618\text{ cm}^{-1}$  in the Raman spectrum) can be assigned to the antisymmetric stretching vibration of the  $\text{COO}^-$  group, similar to other addition compounds of glycine (21, 22). The observed lack of sensitivity of the band to deuteration can be interpreted as confirming this assignment.

As a consequence of the existence of two nonequivalent species,  $\text{CH}_2\text{NH}_3^+\text{COO}^-$  and  $\text{CH}_2\text{NH}_3^+\text{COOH}$ , the bands corresponding to the vibrations of the  $\text{NH}_3^+$  group, together with the expected splitting of all the vibration band into doublets, could, in the extreme case, indicate up to four-fold multiplication. However, the fact of the intense incorporation of the  $\text{NH}_3^+$  groups into the system of hydrogen bonds in the crystal, which always leads to merging of formerly separated vibrations, is in contradiction with this concept. The deformation vibrations of the  $\text{NH}_3^+$  group appears predominantly in the IR spectrum in the  $1600\text{--}1500\text{ cm}^{-1}$  region. The expected splitting is especially apparent for the

antisymmetrical vibration in the low-temperature spectrum. Further marked multiplication can be found for the rocking vibration in the  $1160\text{--}1060\text{ cm}^{-1}$  region.

The presence of glycinium ions ( $\text{CH}_2\text{NH}_3^+\text{COOH}$ ) in the crystal structure is reflected in the bands of the C-O stretching vibration (IR  $1375\text{ cm}^{-1}$ ) and C-O-H in-plane (IR  $1259\text{ cm}^{-1}$ ) and out-of-plane (IR  $935\text{ cm}^{-1}$ , RA  $932\text{ cm}^{-1}$ ) bending vibrations. It is assumed that the  $\nu\text{C-O}$  and  $\delta\text{C-O-H}$  vibrations are highly mixed (22).

The expected splitting of the internal vibrations of the  $\text{HSeO}_3^-$  group (see Table 7) was observed in the spectra in the  $\nu_1$ ,  $\nu_4$ , and  $\nu_5$  modes.

In the Raman spectra of the natural and deuterated compounds, the lattice modes are located in the region below  $300\text{ cm}^{-1}$ . The intense bands at  $\sim 135$  and  $\sim 105\text{ cm}^{-1}$  can once again be assigned to the torsion vibrations of the  $\text{COO}^-$  (15) and C-C (16) groups.

#### *Thermal Behavior of DGSe(IV) and MGSe(IV)*

Crystals of DGSe(IV) and MGSe(IV) are stable in the air up to temperatures of 385 and 363 K, respectively, where they melt and decompose.

Both compounds were further studied by the DSC method from a temperature of 95 K up to temperatures immediately prior to the beginning of the melting process. No thermal effects were observed for any of the substances in the entire temperature interval.

TABLE 10  
 FTIR and FT Raman Spectra of DGSe(IV)

Assignment	IR			Assignment	IR			
	298 K	90 K	Raman		298 K	90 K	Raman	
$\nu$ N-H...O, $\nu$ O-H...O	3230 sh	3230 sh		$\rho$ NH <sub>3</sub> <sup>+</sup>	1161 m	1167 s		
	3140 sh	3130 sh			1147 m	1153 m	1151 w	
	3095 mb	3095 mb	3085 w			1143 m		
$\nu_{as}$ CH <sub>2</sub>	3014 m	3018 m	3014 s		1138 m	1138 w		
			2996 s		1125 m	1131 w	1127 w	
$\nu_s$ CH <sub>2</sub>			2976 s			1111 w		
	2950 mb	n.o. <sup>a</sup>	2958 s	$\gamma$ OHO	1064 m	1077 m		
$\nu$ N-H...O, $\nu$ O-H...O	2880 sb	n.o. <sup>a</sup>	2850 w	$\nu$ C-N	1050 m	1055 m	1052 m	
	2820 s	n.o. <sup>a</sup>		$\gamma$ C-O-H	935 m	940 m	932 w	
		2770 m		$\rho$ CH <sub>2</sub>	921 m	924 m	923 w	
	2740 m	2752 m	2745 w	$\nu$ C-C	899 m	901 m	903 w	
		2662 m			881 m	883 m	883 s	
	2645 m	2650 sh	2650 w	$\nu_s$ Se-O ( $\nu_2$ HSeO <sub>3</sub> <sup>-</sup> )	843 s	844 s	845 vs	
		2577 m		$\nu_{as}$ Se-O ( $\nu_5$ HSeO <sub>3</sub> <sup>-</sup> )	817 s	820 s	809 m	
	2545 m	2556 m				803 sh		
	2450 mb	2463 m			785 sh	795 s	790 w	
	2430 mb	2430 mb		?		733 w		
	2405 mb	2411 m				702 wb		
		2330 w		$\delta$ COO <sup>-</sup>	673 m	674 m	673 w	
		2310 wb	2305 wb		653 w	655 w	653 w	
	$\delta_{as}$ NH <sub>3</sub> <sup>+</sup> + $\tau$ NH <sub>3</sub> <sup>+</sup> $\nu$ O-H...O	2100 w	2119 m		$\nu$ Se-OH ( $\nu_1$ HSeO <sub>3</sub> <sup>-</sup> )	600 s	609 m	605 vs
		2040 wb	2048 m				599 s	596 sh
1985 wb		1994 m		$\omega$ COO <sup>-</sup>	541 s	542 s	541 w	
1945 sh		1945 m			532 sh	535 m		
		1922 m		$\tau$ NH <sub>3</sub> <sup>+</sup>		512 w		
	1905 m			505 m	505 m	505 w		
	1888 m				501 w			
	1865 wb	1874 m		?		461 w		
$\nu$ C=O	1761 m	1767 m	1760 sh	$\rho$ COO <sup>-</sup>	435 w	446 w		
	1735 s	1734 s	1727 w	$\delta$ O-Se-O ( $\nu_4$ HSeO <sub>3</sub> <sup>-</sup> )	414 m	417 m	416 w	
?		1640 sh				413 m		
$\nu_{as}$ COO <sup>-</sup>	1633 m	1631 m		$\delta_{as}$ HO-Se-O ( $\nu_6$ HSeO <sub>3</sub> <sup>-</sup> )		364 m		
	1623 m	1619 m	1618 w	$\delta$ C-C-N			347 m	
$\delta_{as}$ NH <sub>3</sub> <sup>+</sup>	1601 m	1606 m		$\delta_s$ HO-Se-O ( $\nu_3$ HSeO <sub>3</sub> <sup>-</sup> )			318 w	
		1591 sh		lattice modes			300 w	
		1575 m					250 w	
$\delta_s$ NH <sub>3</sub> <sup>+</sup>	1531 s	1534 s	1529 w				222 m	
	1513 s	1515 s					200 m	
sci CH <sub>2</sub>	1437 s	1437 m	1441 m				179 m	
		1430 m	1432 m				160 m	
$\nu_s$ COO <sup>-</sup>	1411 s	1412 s	1409 w				137 s	
		1405 m					125 s	
$\nu$ C-O	1375 s	n.o. <sup>a</sup>					108 s	
$\omega$ CH <sub>2</sub>		1321 s					81 m	
	1313 s	1315 s	1319 m				75 m	
$\delta$ C-O-H	1259 s	1267 s					61 w	
$\delta$ Se-O-H	1240 sh	1250 s					55 w	
		1223 m						

<sup>a</sup>not observed due to nujol bands

**TABLE 11**  
**FTIR and FT Raman Spectra of Deuterated DGSe(IV)**

Assignment	IR	Raman	Assignment	IR	Raman
?	3087 w		$\nu$ CN, $\nu$ CC, $\rho$ ND <sub>3</sub> <sup>+</sup>	955 w	974 m
$\nu_{as}$ CH <sub>2</sub>	3014 m	3015 s	$\delta$ Se–O–D	919 m	
	3000 m	3001 vs	$\nu_s$ Se–O ( $\nu_2$ DSeO <sub>3</sub> <sup>-</sup> )	844 s	851 vs
$\nu_s$ CH <sub>2</sub>	2973 m	2976 vs	$\nu_{as}$ Se–O ( $\nu_5$ DSeO <sub>3</sub> <sup>-</sup> ),	820 s	813 m
	2959 m	2962 vs	$\nu$ CN, $\nu$ CC, $\rho$ ND <sub>3</sub> <sup>+</sup>		
?	2785 wb	2850 w	$\rho$ CH <sub>2</sub> , $\rho$ ND <sub>3</sub> <sup>+</sup>	789 m	793 w
$\nu$ N–D...O, $\nu$ O–D...O	2350 mb	2360 m		779 m	
	2305 sb			760 sh	
	2275 sb	2265 m	?		712 w
	2180 s	2185 m	$\delta$ COO <sup>-</sup>	645 s	647 w
	2140 sb	2130 m		617 w	
	2110 mb		$\nu$ Se–OD ( $\nu_1$ DSeO <sub>3</sub> <sup>-</sup> )	590 s	588 vs
	2025 wb		$\omega$ COO <sup>-</sup>	518 m	513 w
	1958 w	1950 w	$\rho$ COO <sup>-</sup>	484 w	485 w
	1825 w		$\delta$ O–Se–O ( $\nu_4$ DSeO <sub>3</sub> <sup>-</sup> )	425 m	424 w
$\nu$ C=O	1731 s	1725 w	?		374 m
$\nu_{as}$ COO <sup>-</sup>	1632 m	1630 w	$\delta_{as}$ DO–Se–O ( $\nu_6$ DSeO <sub>3</sub> <sup>-</sup> )		360 m
sci CH <sub>2</sub>	1437 m	1435 m	$\delta_s$ DO–Se–O ( $\nu_3$ DSeO <sub>3</sub> <sup>-</sup> )		328 m
$\nu_s$ COO <sup>-</sup> , $\nu$ C–O	1397s	1402 m	$\delta$ C–C–N		309 w
$\omega$ CH <sub>2</sub>		1320 sh	lattice modes		285 w
	1297 s	1300 m			249 w
twi CH <sub>2</sub>	1285 s				237 m
	1277 s	1273 m			200 m
?	1245 m				185 m
$\delta_s$ ND <sub>3</sub> <sup>+</sup>	1189 m				159 s
$\delta_{as}$ ND <sub>3</sub> <sup>+</sup>	1173 m	1170 w			146 s
?	1074 m	1070 w			135 s
$\rho$ CH <sub>2</sub> , $\rho$ ND <sub>3</sub> <sup>+</sup>	1048 w	1036 w			105 s
	1019 w	1018 m			89 s
$\nu$ CN, $\nu$ CC, $\rho$ ND <sub>3</sub> <sup>+</sup>		1001 w			75 s
					62 w

The FTIR spectra (see Figs. 3 and 4 and Tables 8 and 10) were recorded in the temperature interval from 90 to 298 K. The changes found in the low-temperature spectra are a result particularly of the temperature effect, accompanied by narrowing and partial separation of the vibrational bands. In spite of the observed shifts in some bands, it can be stated that a decrease in the temperature of the sample does not lead to any changes in the infrared spectrum that would indicate the occurrence of structural phase transitions.

These conclusions, together with the results of DSC measurements, unambiguously demonstrate that there is no phase transition to a polar phase in the test compounds and thus the existence of ferroelectric properties in the studied temperature interval can be completely excluded for the DGSe(IV) and MGSe(IV) crystals, for reasons of the centrosymmetry of their space groups. This conclusion is also confirmed by the absence of short hydrogen bonds

between the carboxyl groups in the crystal structure of MGSe(IV). This bonding interaction, as mentioned above, plays an important role in the phase transitions of all existing ferroelectric compounds of the TGS type.

#### ACKNOWLEDGMENT

This work was supported by the Grant Agency of the Czech Republic under Grant GA30608.

#### REFERENCES

1. M. I. Kay and R. Kleinberg, *Ferroelectrics* **5**, 45 (1973).
2. S. Sato, *J. Phys. Soc. Japan* **25**, 185 (1968).
3. M. Ichikawa, *Ferroelectrics* **39**, 1033 (1981).
4. J. Ondráček, M. Walzelová, Z. Mička, and J. Novotný, *Acta Crystallogr. C* **48**, 391 (1992).
5. H. Arend and J. J. Connelly, *J. Cryst. Growth* **56**, 642 (1982).

6. P. Narayanan and S. Venkataraman, *J. Cryst. Mol. Struct.* **5**, 15 (1975).
7. G. A. Jeffrey and J. Mitra, *J. Am. Chem. Soc.* **106**, 5546 (1984).
8. A. R. Al-Karaghoul, F. E. Cole, M. S. Lehman, C. F. Miskell, J. J. Verbist, and T. F. Koetzle, *J. Chem. Phys.* **63**(4), 1360 (1975).
9. S. Olejnik, K. Lukaszewicz, and T. Lis, *Acta Crystallogr. B* **31**, 1785 (1975).
10. F. H. Cano and S. Martinez-Carrera, *Acta Crystallogr. B* **30**, 2729 (1974).
11. W. Behrendt and U. W. Gerwarth, in "Gmelin Handbook of Inorganic Chemistry—Selenium" (Supplement, Vol. B1, 8th ed.), p. 241. Springer Verlag, Berlin, 1981.
12. Z. Mička, I. Němec, P. Vojtíšek, and J. Ondráček: *J. Solid State Chem.* **122**, 338 (1996).
13. D. L. Rousseau, R. P. Bauman, and S. P. S. Porto, *J. Raman Spectrosc.* **10**, 253 (1981).
14. W. G. Fateley, N. T. McDevit, and F. F. Bentley, *Appl. Spectrosc.* **25**, 155 (1971).
15. Ch. Destrade, Ch. Garrigou-Lagrange, and M. T. Forel, *J. Mol. Struct.* **10**, 203 (1971).
16. H. Stenbäck, *J. Raman Spectrosc.* **5**, 49 (1976).
17. A. A. Ivanov, E. V. Korolik, N. I. Insarova, and G. K. Ilich, *Zh. Prikl. Spektroskopii* **54**(3), 464 (1991).
18. C. A. Cody, R. C. Levitt, R. K. Khanna, and P. J. Miller, *J. Solid State Chem.* **26**, 293 (1978).
19. K. Nakamoto, in "Infrared and Raman Spectra of Inorganic and Coordination Compounds" (4th ed.), p. 122. Wiley, New York, 1986.
20. P. K. Acharya and P. S. Narayanan, *Spectrochim. Acta A* **29**, 925 (1973).
21. R. K. Khanna, M. Horak, and E. R. Lippincott, *Spectrochimica Acta* **22**, 1759 (1966).
22. R. K. Khanna, M. Horak, and E. R. Lippincott, *Spectrochimica Acta* **22**, 1801 (1966).
23. V. Winterfeldt, G. Schaack, and A. Klöpperpieper, *Ferroelectrics* **15**, 21 (1977).
24. Z. Mička, M. Daněk, J. Loub, B. Strauch, J. Podlahová, and J. Hašek, *J. Solid State Chem.* **77**, 306 (1988).
25. M. R. Srinivasan, H. L. Bhat, and P. S. Narayanan, *Ferroelectrics* **46**, 191 (1983).
26. L. Santra, A. L. Verma, P. K. Bajpai, B. Hilczler, and V. Huong, *J. Phys. Chem. Solids* **55**, 405 (1994).
27. P. Shuster, G. Zundel, and C. Sandorfy, in "The Hydrogen Bond," Vol. II, p. 575. North Holland, Amsterdam, 1976.
28. G. M. Sheldrick, "SHELXL 93," University of Göttingen, 1993.
29. "International Tables for X-Ray Crystallography," Vol. IV. Kynoch Press, Birmingham, 1974.
30. V. Petříček and M. Dušek, "JANA 96—Crystallographic Computing System." Institute of Physics, Czech Academy of Science, 1996.
31. H. Nardelli, "PARST, A System for Computer Routines for Calculating Molecular Parameters from Results of Crystal Structure Analysis." University of Parma, 1982.
32. B. Clegg, "PLUTO." University of Göttingen, 1978.